Gridless Solution Method for Two-Dimensional Unsteady Flow

WANG Gang, SUN Ying-dan, YE Zheng-yin
(College of Aeronautics, Northwestern Polytechnic University, Xi'an 710072, China)

Abstract: The main purpose of this paper is to develop a gridless method for unsteady flow simulation. A quadrantal point infilling strategy is developed to generate point and combine clouds of points automatically. A point-moving algorithm is introduced to ensure the clouds of points following the movements of bodyboundaries. A dual time method for solving the two-dimensional Euler equations in Arbitrary Lagrangian-Eulerian (ALE) formulation is presented. Dual time method allows the real-time step to be chosen on the basis of accuracy rather than stability. It also permits the acceleration techniques, which are commonly used to speed up steady flow calculations, to be used when marching the equations in pseudo time. The spatial derivatives, which are used to estimating the inviscid flux, are directly approximated by using local least-squares curve method. An explicit multistage Runge-Kutta algorithm is used to advance the flow equations in pseudo time. In order to accelerate the solution to convergence, local time stepping technique and residual averaging are employed. The results of NACA0012 airfoil in transonic steady flow are presented to verify the accuracy of the present spatial discretization method. Finally, two AGARD standard test cases in which NACA0012 airfoil and NACA64A010 airfoil oscillate in transonic flow are simulated. The computational results are compared with the experimental data to demonstrate the validity and practicality of the presented method.

Key words: computational fluid dynamics; gridless method; dual time method; unsteady flow; Euler equation

一种计算非定常二维流动的无网格算法. 王 刚, 孙迎丹, 叶正寅. 中国航空学报(英文版), 2005, 18(1): 8-14.

摘 要: 主要目的是发展一套求解非定常流动的无网格算法。计算区域的离散方面,提出了一种按区域进行填充布点的点云自动生成方法;发展了一种点云的运动技术来实现离散点云对物面边界的随体运动;在点云离散的基础上,采用最小二乘法求解矛盾方程的方法来求取空间导数,进而获得数值通量;采用双时间方法进行时间离散推进,其中物理时间迭代采用二阶隐式格式,伪时间迭代采用四步龙格-库塔显式格式,为了加速收敛,在伪时间迭代中采用了当地时间步长和隐式残值光顺等加速收敛措施。最后,利用本文算法模拟了NACA0012翼型和NACA64A010翼型的跨音速非定常流动,并将计算结果与实验测量结果进行了对比分析,验证了上述方法的正确性和实用性。

关键词: 计算流体力学; 无网格方法; 双时间方法; 非定常流; Euler 方程
文章编号: 1000-9361(2005)01-0008-07 中图分类号: V211.3 文献标识码: A

According to the discretization manners of computational region, numerical algorithms in computational fluid dynamics (CFD) can be divided into two rough sorts: the classical grid methods and the burgeoning gridless methods[1-5] in recent years. In gridless methods, clouds of points which are composed of the point itself and its neighbor points, are adopted to substitute for grid cells. The spatial derivatives are directly determined by using local least-squares curve fits over each cloud of points. Gridless methods have much geometrical flexibility for computing with complex configurations because they throw off the grid cell thought and break away from the restrictions of the grid quality and topological structure.

During using grid algorithm to calculate the unsteady flow, the body-fitted dynamic grid technique[6-8] must be used to simulate unsteady mo-

Received date: 2004-04-21; Revision received date: 2004-07-31
Foundation item: The Doctorate Creation Foundation of Northwestern Polytechnic University

tions of body boundaries. But with the restrictions of the grid quality and the grid topological structure, it is very difficult to use moving grids method in the conditions of body boundaries moving in large extent. As mentioned above, gridless methods have no restrictions of grid skewness and stretching distortions, thus, they have distinct advantages for unsteady flow calculation. However, previous researches on gridless solution methods were mainly concerned with steady flow.

The main purpose of this paper is to develop a gridless method for unsteady flow simulation. A quadrant point infilling strategy is developed to generate point and combine clouds of points automatically. A point moving algorithm is introduced to ensure the clouds of points following the movements of body boundaries. The spatial derivatives, which are used to estimating the inviscid flux, are directly approximated by using local least-squares curve method. A dual time method[7] for solving the two-dimensional Euler equations in Arbitrary Lagrangian-Eulerian (ALE) formulation is presented. In this approach, an implicit second-order time discretisation is used in the physical time marching procedure, the pseudo time integration is carried out by an explicit four-step Runge-Kutta scheme and is accelerated by local time stepping and implicit residual smoothing. The results of NACA0012 airfoil in transonic steady flow are presented to verify the accuracy of the present spatial discretization method. Finally, two AGARD standard test cases[9, 10] in which NACA0012 airfoil and NACA64A010 airfoil oscillate in transonic flow are simulated. The computational results are compared with the experimental data to demonstrate the validity and practicality of the presented method.

1 Generation and Moving Technique for Clouds of Points

In gridless method, each discrete point in the computational field has its own cloud of points. As shown in Fig. 1, the point cloud of point i is composed of the point i itself and its neighbor points (the points in the circle). During the flow solving process, spatial derivatives of point i are evaluated by a least-squares fit algorithm in the point cloud of point i. The following is the basic idea of the technique for generating clouds of discrete points automatically.

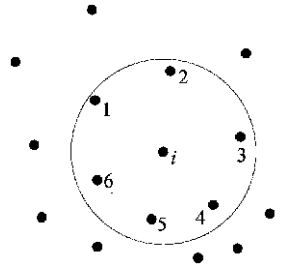

Fig. 1 Sketch map for the framework of the cloud of point i

First, all kinds of the boundaries (body boundaries and far field, *etc*) in the flow computational field are compartmentalized into the form of discrete points. For an arbitrary discrete point i, according to the given background information, the searching radius r of discrete point i in the flow computational field can be ascertained. Then, the searching region for the cloud of the point i can be defined as a circle within the radius of r from the point i. Especially, the searching region is a fan-shaped region if point i is on the boundary. The searching region of point i can be compartmentalized into several sub-regions on the principle of keeping the fan-shaped angles equivalent (shown in Fig. 2). Generally, if the point is in the flow computational field, the searching region is recommended to be divided into six sub-regions, and if the point is on the boundary, four sub-regions are enough.

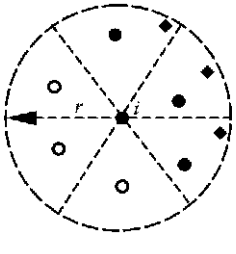

Fig. 2 Sketch map for generating the cloud of point i by using quadrant point infilling strategy

Then, search the point in each sub-region, if there have been already one or more discrete points in a sub-region, the point having the shortest dis-

tance to point i should be added to the cloud of point i, just like the solid points shown in Fig. 2. If there is no point in a sub-region, a new point should be located at the site that is on fan-shaped angle bisector of this sub-region and is $0.5r$ away from the point i. And then the new points (hollow points shown in Fig. 2) should be added to the cloud of point i. Repeat the above process until the cloud of every point in the computational field has been formed.

In unsteady flow computation, in order to simulate the relative movement of body boundaries, it is requested that clouds of discrete points have the ability of moving with the body boundaries. Hence, a point moving algorithm is developed in the following description. Take point i in computational field as an example, its displacement $\Delta \boldsymbol{r}_i$ in one time step is determined by

$$\Delta \boldsymbol{r}_i = \Delta \boldsymbol{r}_j \sin\left(\frac{d_{ij}}{D_j}\pi\right) \tag{1}$$

where the subscript j is the index of boundary point which is the nearest point away from point i, d_{ij} is the distance from point i to point j, D_j is the shortest distance from point j to the other closed boundary curve and $\Delta \boldsymbol{r}_j$ is the displacement of point j. It is easy to determine $\Delta \boldsymbol{r}_j$ during the course of computation because point j is on the boundary. In the same way, the displacement of an arbitrary point in the flow field also can be determined as Eq. (1).

2 Unsteady Flow Numerical Simulation Method

2.1 Governing equations

The Euler equation in Arbitrary Lagrangian-Eulerian (ALE) differential form for the Cartesian coordinate system can be described as follows:

$$\frac{\partial \boldsymbol{Q}}{\partial t} + \frac{\partial \boldsymbol{E}}{\partial x} + \frac{\partial \boldsymbol{F}}{\partial y} = \boldsymbol{0} \tag{2}$$

where

$$\boldsymbol{Q} = (\rho \quad \rho u \quad \rho v \quad e_0)^{\mathrm{T}},$$

$$\boldsymbol{E} = \{\rho(u - u_{\mathrm{P}}) \quad \rho u(u - u_{\mathrm{P}}) + p \quad \rho v(u - u_{\mathrm{P}}) \quad e_0(u - u_{\mathrm{P}}) + pu\}^{\mathrm{T}},$$

$$\boldsymbol{F} = \{\rho(v - v_{\mathrm{P}}) \quad \rho u(v - v_{\mathrm{P}}) \quad \rho v(v - v_{\mathrm{P}}) + p \quad e_0(v - v_{\mathrm{P}}) + pv\}^{\mathrm{T}}$$

The equations are non-dimensionalized with a reference density ρ_∞ and a speed of sound a_∞. Here ρ, u, v, p and e_0 represent the gas density, velocity components in x and y directions, pressure and total energy per unit volume. On the perfect gas assumption, the pressure p can be calculated from the equation of state $p = (\gamma - 1) \cdot \left[e_0 - \frac{\rho}{2}(u^2 + v^2)\right]$, where γ is the ratio of specific heats of the fluid and typically taken as 1.4 for air, u_{P} and v_{P} represent velocity components in x and y directions of the discrete points.

2.2 Numerical discretization

When gridless method is applied for the spatial discretization of the governing equations, where the shoe pinches is to determine the spatial derivative of the conserved variable $\boldsymbol{Q}$. The numerical flux $\left(\frac{\partial \boldsymbol{E}}{\partial x} + \frac{\partial \boldsymbol{F}}{\partial y}\right)$ can be obtained by the derivative calculating principle of compound function.

Suppose the value of ρ has been known on every point, considering the cloud of a point shown in Fig. 1, the spatial derivatives $\frac{\partial \rho}{\partial x}$ and $\frac{\partial \rho}{\partial y}$ can be computed by the following method. If n is the number of discrete points in the cloud of point i, then a system of $n-1$ linear equations with the unknown variables $\frac{\partial \rho}{\partial x}$ and $\frac{\partial \rho}{\partial y}$ can be obtained by a first-order accuracy Taylor series expansion about point i

$$\rho_j = \rho_i + \left.\frac{\partial \rho}{\partial x}\right|_i (x_j - x_i) + \left.\frac{\partial \rho}{\partial y}\right|_i (y_j - y_i) \quad (j = 1, 2 \cdots, n-1) \tag{3}$$

where the subscript j is the index number of the discrete points except for point i in the cloud of point i. According to the construction manner of the cloud of points, the total number of discrete points in the cloud should be more than three, hence the above equations are inconsistent in fact. In order to obtain the approximate solution of the inconsistent Eq. (3), a linear least-squares method is used. It can be proved that the algorithm of calculating spatial derivative in this paper is equiva-

lence to the method introduced in Ref. [1, 3].

According to the above method, the numerical flux $\boldsymbol{R}_i = \left.\frac{\partial \boldsymbol{E}}{\partial x}\right|_i + \left.\frac{\partial \boldsymbol{F}}{\partial y}\right|_i$ in Eq. (2) can be derived from the derivative calculating principle of compound function by using the spatial derivative of the conserved variables ρ, ρu, ρv and e_0 on the cloud of points. So the semi-discretization form of Eq. (2) on point i can be expressed as

$$\frac{\mathrm{d}\boldsymbol{Q}_i}{\mathrm{d}t} + \boldsymbol{R}_i = \boldsymbol{0} \tag{4}$$

Since the method of the present work is essentially non-dissipative, additional artificial dissipation terms are required to prevent the tendency for spurious even and odd point oscillations and to ensure numerical stability in the course of spatial discretization. Following the method of Ref. [3], artificial dissipation terms are added to Eq. (4) for point i, then it becomes

$$\frac{\mathrm{d}\boldsymbol{Q}_i}{\mathrm{d}t} + \boldsymbol{R}'_i = \boldsymbol{0} \tag{5}$$

where $\boldsymbol{R}'_i = \boldsymbol{R}_i - \boldsymbol{D}_i$, $\boldsymbol{D}_i$ are the artificial dissipation terms.

For inviscid flow, the flow tangent conditions at the solid boundary points are imposed by setting the slip velocities on the boundary faces and eliminating the normal velocity component. In the far field, one dimensional characteristic analysis based on Riemann invariants is used to determine the values of the flow variables on the out boundary of the computational domain.

2.3 Time integration

In a full implicit time concept, time derivatives in Eq. (5) are discretized by second-order backward difference method, then Eq. (5) becomes as

$$3\boldsymbol{Q}_i^{n+1} - 4\boldsymbol{Q}_i^{n} + \boldsymbol{Q}_i^{n-1}/2\Delta t + \boldsymbol{R}'_i(\boldsymbol{Q}_i^{n+1}) = \boldsymbol{0} \tag{6}$$

A dual-time method is introduced to advance the Eq. (6) in real time layer, the derivative terms of conserved variables with respect to pseudo time, τ is added to the left side of Eq. (6). By using the denotation of $\boldsymbol{R}_i^*(\boldsymbol{Q}_i^{n+1}) = (3\boldsymbol{Q}_i^{n+1} - 4\boldsymbol{Q}_i^{n} + \boldsymbol{Q}_i^{n-1})/2\Delta t + \boldsymbol{R}'_i(\boldsymbol{Q}_i^{n+1})$, Eq. (6) can be written as

$$\mathrm{d}\boldsymbol{Q}^{n+1}/\mathrm{d}\tau + \boldsymbol{R}_i^*(\boldsymbol{Q}_i^{n+1}) = \boldsymbol{0} \tag{7}$$

An explicit four-stage Runge-Kutta algorithm is used to advance the flow equations in pseudo time, in which the solution is advanced from pseudo-time level $n\Delta\tau$ to level $(n+1)\Delta\tau$, and can be written as

$$\begin{aligned} &\boldsymbol{Q}^{(0)} = \boldsymbol{Q}_i^n \\ &\boldsymbol{Q}^{(m)} = \boldsymbol{Q}^{(0)} - \alpha_m \Delta\tau_i \boldsymbol{R}_i^*(\boldsymbol{Q}^{(m-1)}) \text{ for } m = 1 \text{ to } 4 \\ &\boldsymbol{Q}_i^{n+1} = \boldsymbol{Q}^{(4)} \end{aligned} \tag{8}$$

where the coefficients

$$\alpha_1 = 1/4,\ \alpha_2 = 1/3,\ \alpha_3 = 1/2,\ \alpha_4 = 1.$$

The major disadvantage of explicit schemes is that the time step $\Delta\tau_i$ is restricted by the Courant-Friedrichs-Lewy (CFL) stability condition. In order to accelerate the solution to convergence, local time stepping technique and implicit residual averaging technique are employed in the pseudo time-integration.

The local time step $\Delta\tau_i$ of discrete point i is given by the following equation

$$\Delta\tau_i = \min\left[\Delta\tau'_i, \frac{2\Delta t}{3}\right] \tag{9}$$

where

$$\Delta\tau'_i = \frac{C_{\mathrm{CFL}}}{n-1}\sum_{k=1}^{n-1} 1/\left[|u_i/(x_i - x_k)| + |v_i/(y_i - y_k)| + a_i\sqrt{1/(x_i - x_k)^2 + 1/(y_i - y_k)^2}\right],$$

C_{CFL} denotes the coefficient of CFL, a_i is the local sound speed at point i, the subscript k is the index number of discrete points which belong to the cloud of point i.

Residual averaging is another technique to accelerate the solution to convergence. This technique extends the region of stabilization, and then increase the maximum value of time stepping permitted in the pseudo-time integration. In gridless method, let R_i represent the residual of point i, a new residual can be given by

$$R'_i = R_i + \varepsilon\left[\sum_{k=1}^{N}(R'_k - R'_i)\right] \tag{10}$$

where ε is the coefficient of residual averaging, and its recommended value is a number between 0.2 to 0.5. This technique of implicit residual averaging allows the CFL number to be increased about two

times larger than the unsmoothed value.

3 Results

The spatial discretization accuracy of the present gridless method is evaluated by performing the steady flow calculation about transonic flow around the NACA 0012 airfoil. In order to further understand the characteristics of the current gridless method in the case of unsteady flow, the unsteady flow simulations for NACA0012 airfoil and NACA64A010 airfoil oscillations in pitch about quarter chord in transonic flow are conducted. For each test case, the criterion of convergence for the pseudo-time integration process is the maximum value of residual decrease to the order of 10^{-6}.

3.1 Transonic steady flow around NACA0012 airfoil

To give an evaluation for numerical accuracy of the present gridless method, a transonic steady flow at $Ma = 0.80$ and $\alpha = 1.25°$ around NACA0012 airfoil is computed. The close-up view of the field points is displayed in Fig. 3. There are

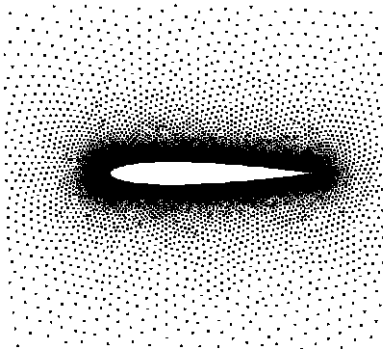

Fig. 3 Partial view of points distribution around NACA0012 airfoil

200 points distributed on the boundary of airfoil and 6145 points distributed on the whole computational field. As shown in Fig. 4, the calculated surface pressure coefficient distributions compare well with the experimental data. In this test case, both the strong shock on the upper surface and the weak shock on the lower surface are well captured. Therefore, the gridless method presented in this paper has nicer capability to resolve flow discontinuity.

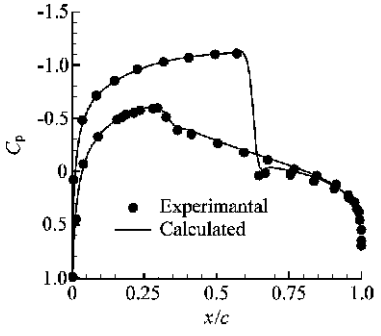

Fig. 4 Pressure coefficient distributions for transonic flow around NACA0012 airfoil

3.2 Unsteady transonic flow around oscillating NACA0012 airfoil

One of the standard test cases for the NACA0012 airfoil is considered. The computed results are compared with the classical AGARD experiment data[9]. In this test case, the NACA0012 airfoil oscillates in pitch about its quarter chord and the instantaneous angle of attack $\alpha(t)$ is given by

$$\alpha(t) = \alpha_0 + \alpha_m \sin(\omega t) \qquad (11)$$

where α_0 is the mean incidence, α_m is the amplitude of pitching angle, the angular frequency ω is related to the reduced frequency k by the relationship $k = \omega c/(2V_\infty)$, where c is the airfoil chord length and V_∞ is the free stream speed. The test case is simulated with the following conditions: $Ma = 0.755$, $\alpha_0 = 0.016°$, $\alpha_m = 2.51°$, $k = 0.0814$.

The distribution of cloud of points in the former test case is taken as the initial point distribution of current case. The computation is carried out using 72 real-time steps in one oscillation cycle. The average run time per oscillating period is nearly 0.3 h, and the number of pseudo-time steps for each real-time step is approximate to 300. Compared with the experimental data, the calculated instantaneous pressure coefficient distributions at four points in time during the forth circle of motion are shown in Figs. 5(a)-5(d). In these figures, $\Phi(t)$ denotes the phasic angle of oscillation at that moment. Instantaneous lift coefficients C_l and instantaneous moment coefficients C_m *vs* the instantaneous angles of attack are plotted in Fig. 6 and Fig. 7. In these two figures, the calculated results of the present approach agree well with the experi-

mental data and the related numerical results[6].

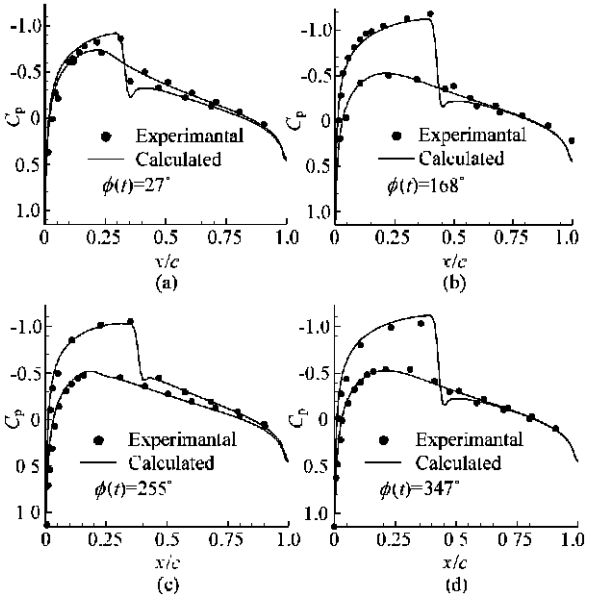

Fig. 5 Instantaneous surface pressure coefficient distributions for NACA 0012 airfoil in the forth circle of motion

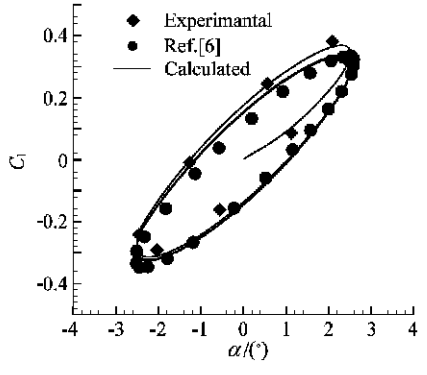

Fig. 6 Lift coefficients *vs* the instantaneous angle of attack

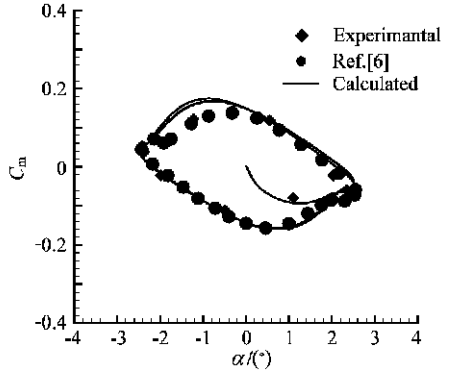

Fig. 7 Moment coefficients *vs* the instantaneous angle of attack

3.3 Unsteady flow around oscillating NACA64-A010 airfoil

To further understand the properties of the present gridless method for unsteady flow simulation, the transonic flow around NACA64A010 airfoil oscillation in pitch about its quarter chord is simulated. The instantaneous angle of attack can distribution of points around the NACA64A010 airfoil is also given by Eq. (11) and with the following conditions: Ma= 0.796, α_0= 0.0°, α_m= 1.01°, k= 0.202.

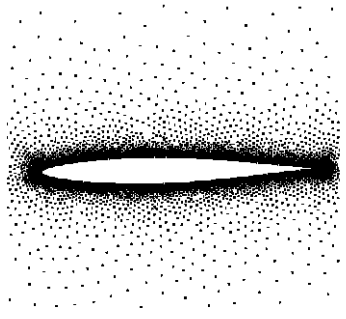

Fig. 8 Partial view of points distribution around the NACA64A010 airfoil

Distribution of points around the NACA64-A010 airfoil is shown in Fig. 8. There are 270 points distributed around the airfoil and 5681 points distributed in the whole computational field. In this case, 120 time steps are given for one oscillation circle during the computation because the angle frequency in here is higher.

Instantaneous lift coefficients C_l *vs* the instantaneous angle of attack are plotted in Fig. 9. The

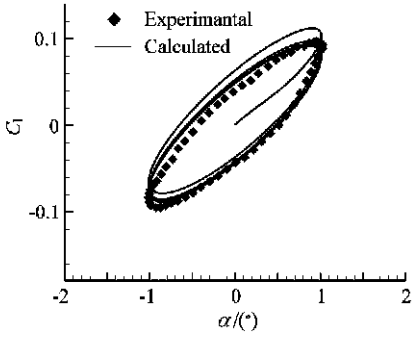

Fig. 9 Lift coefficients *vs* the instantaneous angle of attack

present results compare well with the experimental data[10]. The in-phase and in-quadrature components of the 1st harmonic of unsteady surface pressure coefficients in the forth circle of oscillation are shown in Fig. 10 and compared with the experimental results there.

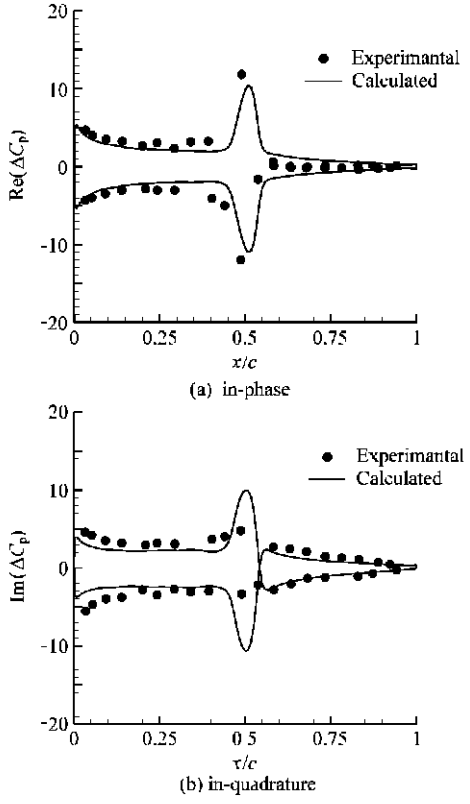

Fig. 10 The in-phase and in-quadrature components of the 1st harmonic of unsteady surface pressure coefficients in the forth circle

4 Conclusions

In this paper, a gridless algorithm has been developed to simulate unsteady flow. A quadrantal point infilling strategy is employed to generate the cloud of points. A point moving algorithm is introduced to ensure the clouds of points following with the movement of body boundaries. The spatial derivatives are directly determined by using local least-squares curve fits in each cloud of points, and then numerical flux can be obtained. A dual time method is used to advance the flow equations in time. The computation of NACA0012 airfoil in transonic steady flow proves the accuracy of spatial discretization in the present gridless method. The unsteady flow of NACA0012 airfoil and NACA64A010 airfoil oscillation in pitch about their quarter chord are simulated and the results are in good agreement with the experimental data. These test cases demonstrate the validity and practicality of the present method. The present research has made primary foundation for applying the gridless method to simulate unsteady flow. The present method can also be directly extended to two-dimensional unsteady viscous flow and three-dimensional unsteady flow.

References

[1] Barth T J. A gridless Euler/Navier-Stokes solution algorith for complex aircraft applications[R]. AIAA Paper 93-0333, 1993.

[2] Morinishi K. A gridless type solution for high Reynolds number multielement flow fields[R]. AIAA Paper 95-1856, 1995.

[3] Liu J L, Su S J. A potentially gridless solution method for the compressible Euler/Navier-Stokes equations[R]. AIAA Paper 96-0526, 1996.

[4] Onate E, Idelsohn S. A mesh-free finite point method for advective-diffusive transport and fluid flow problems [J]. Computational Mechanics, 1998, 21 (2): 283-292.

[5] Lohner R, Sacco C, Onate E, *et al*. A finite point method for compressible flows [J]. International Journal for Numerical Methods in Engineering, 2002, 53 (8): 1765-1779.

[6] Hwang C J, Yang S Y. Locally implicit total variation diminishing schemes on mixed quadrilateral-triangular meshes [J]. AIAA Journal, 1993, 31 (11): 2008-2015.

[7] Gaitonde A L. A dual-time method for the solution of the unsteady Euler equations [J]. Aeronautical Journal, 1994, 98 (10): 283-291.

[8] Lu Z L. Generation of dynamic grids and computation of unsteady transonic flows aroune assemblies [J]. Chinese Journal of Aeronautics, 2001, 14(1): 1-5.

[9] Landon R H. NACA 0012 oscillatory and transient pitching [R]. AGARD Report 702, AGARD, 1982. Dataset 3.

[10] Davis S S. NACA 64A010 (NASA Ames model) oscillatory pitching[R]. AGARD Report 702, AGARD, 1982. Dataset 2.

Biographies:

WANG Gang Born in 1977 in Hubei province, a graduate student for the doctoral degree in Northwestern Polytechnic University. He is researching in computational fluid dynamics.
Tel: 029-88491342, E-mail: wanggang@nwpu.edu.cn

SUN Ying-dan Born in 1979 in Liaoning province, a post-graduate student in College of Aeronautics of Northwestern Polytechnic University. She is working on the gridless method in CFD.
Tel: 029-88493955, E-mail: sunyingdan2002@tom.com

YE Zheng-yin Born in 1963 in Hubei province, professor of Northwestern Polytechnic University. He is researching in CFD and aero-elastic dynamics.
Tel: 029-88491374, E-mail: yezy@nwpu.edu.cn